



NOVEL GEAR DIAGNOSIS TECHNIQUE BASED ON SPECTRAL KURTOSIS

Harish Chandra and Len Gelman

Cranfield University, School of Aerospace Transport and Manufacturing, Bedford, United Kingdom
email: l.gelman@cranfield.ac.uk

In this paper, a new thresholding technique used for diagnosis of gearbox pitting tooth faults is introduced. The diagnosis procedure involves in estimation of the Time Synchronous Average (TSA) signal and the gear residual signal, and then the Spectral Kurtosis optimal filter is estimated using the proposed thresholding procedure. By considering overlapping among the TSA segments, several realizations of the TSA signal are estimated. It is important that the SK estimated over the realizations should be consistent. The statistical SK thresholding procedure presented in literature is used for comparing the performance of the proposed approach. A three stage diagnosis decision making technique based on weighted majority rule is used for final diagnosis.

1. Introduction

Rotating machinery components such as gearboxes are subject to heavy operating conditions. It is very important to develop online monitoring tools to access the health of the gearboxes. During the past several years Spectral Kurtosis based fault diagnosis has been successfully employed for diagnosis of rolling element bearings and gearboxes [1, 2]. For stationary vibration components the spectral kurtosis is effectively zero [3]. For non-stationary vibration components the SK shows a larger frequency band. If multiple faults exist, multiple frequency bands may be generated [4]. Since the non-stationary vibration corresponds to the damage, the SK can be used as a filter to separate the signal corresponding to the damage.

For diagnosis of gearboxes, essential pre-processing steps such as TSA estimation and gear residual signal are very useful. Based on literature survey many researchers suggested the use of Time Synchronous Averaged (TSA) signal and gear residual signal for diagnosis of faults. The TSA signal can be estimated from the raw vibration data either by using a tachometer (speed sensor) or by using an automated procedure [5]. The gear residual signal is an outcome of TSA signal. The gear residual signal does not contain interfering components and the gear mesh frequency components. The gear residual signal is estimated from TSA signal by removing the mesh harmonics. In this paper the automated procedure is employed. The spectral kurtosis will be estimated for all the gear residual signal realizations. By considering overlapping about the TSA segments, several realizations of the TSA signal are estimated.

2. Spectral Kurtosis: Theory

The spectral kurtosis is interpreted as an adaptive technique used to determine the most suitable frequency band for extraction of the impact related non-stationary component of the signal. It was shown in [1] that the SK of the sum $r(t) = x(t) + n(t)$, where $x(t)$ is the nonstationary component and $n(t)$ is the stationary Gaussian noise, can be related to the SK of the non-stationary part $x(t)$ by,

$$K_r(f) = \frac{K_x(f)}{[1+\rho(f)]^2} \quad (1)$$

where, $K_r(f)$ is the spectral kurtosis of the sum $r(t)$, $K_x(f)$ is the spectral kurtosis of the non-stationary component $x(t)$, and $\rho(f) = \frac{S_n(f)}{S_x(f)}$ the ratio of the power spectral densities of $n(t)$ and $x(t)$ reflecting the noise-to-signal ratio with respect to the frequency.

2.1 Proposed Spectral Kurtosis thresholding technique

In this section, the description for the proposed consistency based spectral kurtosis thresholding methodology is presented. Considering overlapping between the TSA segments will yield realizations of the TSA signal. The consistency of the SK estimated along the realizations will confirm that the SK band is not produced due to any random event or any measurement error. Due to poor choice of the threshold, for some of the realizations the spectral kurtosis will be zero. In this paper, to ensure the consistency of the SK over the realizations a consistency parameter (p) is formulated. The consistency parameter (p) will indicate the percentage of number of realizations for the estimated SK is non-zero (or consistent).

To estimate the consistency parameter, a search algorithm is developed to identify SK realizations with non-zero SK amplitude. If an SK realization is found inconsistent, a value of 0 is assigned to that realization or else to a consistent SK realization a value of 1 is assigned. For each SK realization the consistency matrix with digits 1 or 0 is recorded as vector. To obtain the consistency parameter the following equation is used.

$$p = \frac{\sum CM}{N_{real}} \times 100 \quad (2)$$

Where p is the consistency parameter in (%), CM is the consistency matrix with digits 1 or 0 for consistent and inconsistent SK realizations and N_{real} is the total number of realizations.

For each threshold choice the consistency parameter (p) will be estimated. The Weiner filter estimated using the SK threshold is as presented below,

$$W(f) = \begin{cases} \sqrt{K_r(f)} & \text{for } K_r(f) > SK_{Th} \\ 0 & \text{other wise} \end{cases} \quad (3)$$

Where K_r the Spectral Kurtosis of the gear is residual signal and s is the threshold. The threshold SK_{Th} is chosen based on the following criteria,

1. After extracting the realizations of the gear residual signal from the TSA signal the SK is estimated, the SK estimated must be consistent for all the realizations. The consistency parameter should be 100% for a chosen threshold.
2. If the consistency parameter (p) is less than 100% a threshold lower than the previous threshold will be tested for consistency
3. For every realization the SK frequency band must correspond to same frequency band produced by the SK.

To obtain a reliable diagnosis the fault features corresponding to undamaged and the damaged data are to be compared. Tools such as Fishers Criterion (FC), Anomaly detection and Decision making algorithms are used to either estimate the separation between the undamaged and damaged fault features or estimate the probability of correct diagnosis. In this paper the same threshold estimated for damaged data is considered for processing undamaged data for comparison and estimating the separation between the fault features.

3. Experimental results

3.1 Test rig 1

Test rig 1 is a multistage stage industrial gearbox. This test rig consists of two similar gearboxes (Gearbox A and B) which are connected back to back through a shaft. A hook joint is used to connect the two back to back gearboxes. The helical gears are denoted as Z_1 , Z_2 , Z_3 and Z_4 with teeth 14, 46, 13 and 54 respectively. The speed corresponding to the three shafts (Shaft 1, 2 and 3) is 20 Hz, 6.09 Hz and 1.4 Hz respectively. Tri-axial accelerometers A1 and A2 are mounted on the gear-

box at locations closer to shaft 1 and shaft 2 respectively. The vibration data is captured at different instances of time, before and after damaged. Total 9 vibration data sets are captured after 0 hours, 1 hour, 15hours, 18 hours, 34 hours, 40 hours, 58 hours and 60.5 hours and are denoted as run#1 to run#9 consecutively. The data corresponding to Run #1, Run#2 and Run#3 represent the undamaged data sets. After 58 hours of operation, the gear teeth are visually investigated to identify the presence of damage. At that instant, the pitting on the pinion Z3 was noticed. Thus the data for Runs #8 and #9 represent the damaged response of the gearbox. The relative pitting damage percentage estimates were calculated from the area of the damaged surface relative to the surface of the whole tooth. The data acquired between 15 to 58 hours i.e. run #4 to run #7 are vibration data sets corresponding to transition from undamaged to damaged conditions. Torque information was also noted for every run. Average level of torque noted was ~900 N.m for all the test runs. The schematic of the test rig is presented in Fig. 1

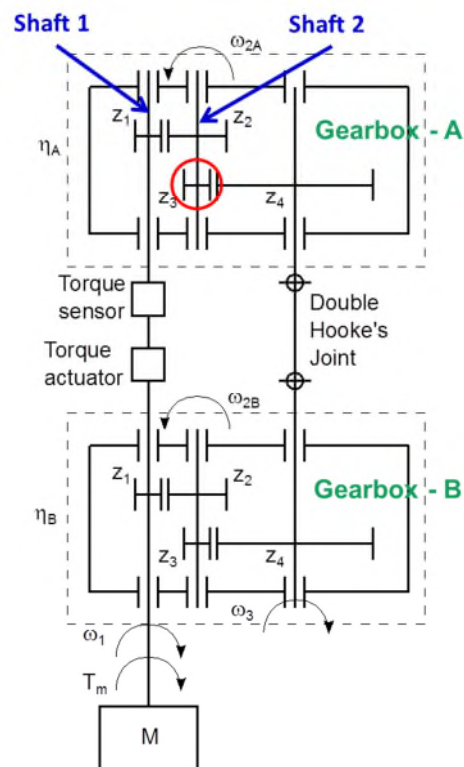


Figure 1: Schematic of the test rig.

3.1.1 Diagnosis results

Prior to SK filtering, the raw vibration signal needs to be pre-processed in order to isolate vibrations related to individual components and remove interfering components. Therefore, the SK is estimated by processing the gear residual signal, which is obtained by resampling the vibration signal from time into the angular domain, time synchronous averaging and cleaning of periodic gear mesh components. In this paper an automated method is used for estimating the TSA signal [5]. The accuracy of the estimated technique depends on the accuracy of the estimated input nominal speed. The input speed is accurately estimated as ~1200 rpm for both undamaged and damaged vibration data. The TSA signal and its corresponding frequency spectrum are as presented in Figure 2(a).

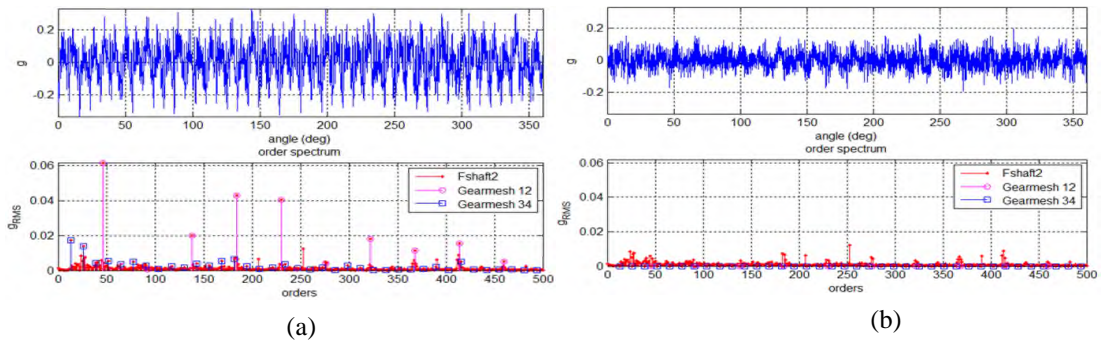


Figure 2: Response and its order spectrum (a) Time synchronous averaged (TSA)
(b) Gear residual signal.

In Figure 2, for the frequency spectrum of TSA and gear residual signals, the gearmesh12 refers to GMF corresponding to Z_1 and Z_2 gears; similarly gearmesh 34 refers to GMF corresponding to Z_3 and Z_4 . It can be observed from Figure 2(a), the spectrum of the TSA response contains the GMF components corresponding to both stages of the gearbox. By filtering the gear mesh frequencies as shown in Figure 2(b-bottom) and reconstructing using inverse Fourier transform the gear residual is obtained. Thus the gear residual clearly contains no spectral components corresponding gear mesh frequencies. It contains information corresponding to damage.

3.1.2 SK thresholding

As shown in Figure , the Spectral Kurtosis for undamaged data for 5 realizations the frequency bands representing the fault are absent. However, clearly for damaged data case a frequency band with centre frequency around 767Hz is observed. The SK results are presented for half mesh frequency resolution ($4 \times GMF = 317Hz$).

The SK estimated using statistical thresholding procedure as explained in [1] is applied to the SK estimates presented in Figure . For different levels of consistency parameter the Wiener filters using proposed SK thresholding technique are presented in Figure 3. As shown in Figure 3(a), the chosen SK threshold is 3.7 and the estimated consistency parameter for this case is $p = 77.77\%$. For damaged case among 18 SK realizations only 14 realization show consistent SK values other 4 realizations have projected poor diagnosis results.

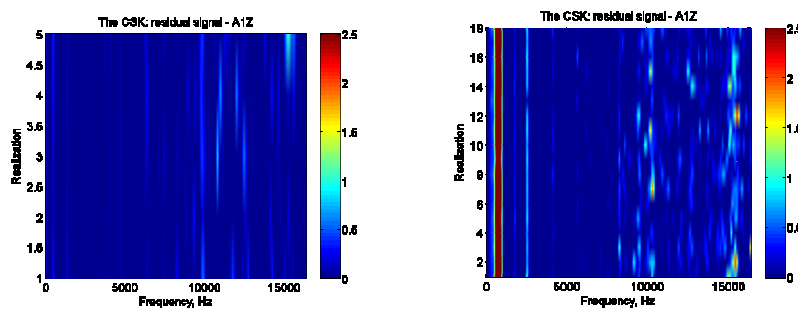


Figure 3: Spectral Kurtosis for undamaged (left) and damaged data sets (right).

For consistency parameter equal to $p = 88\%$, the SK optimal filter is as shown in Figure 3(b). Even this case is not an optimal choice of threshold for performing diagnosis decision making, because the consistency level is poor. For SK Threshold 3.5 and 2 the consistency parameter is estimated as $p = 100\%$ and the results are as shown in Figure 3(c). For the case as shown in Figure 3(c), the consistency is 100%. However, the narrow band case will have higher SK threshold and tends to maximize the SK estimate. The undamaged fault features and damaged fault features are clearly separated for all consistency levels. However for high consistency levels the feature separation is very high and will yield no false alarms.

Based on the statistical SK thresholding technique available in literature [1, 2] (as presented in section 2.2), the SK filter and the corresponding fault features estimated for 1% probability of normal distribution are as presented in Figure 5(a and b) respectively. The Fault features are separated, however this choice of thresholding technique yields inconsistent frequency bands and unstable diagnosis decisions. Using the proposed method the estimated SK threshold is 3.5 for which the consistency is maximum for CSK technique. The SK estimated is consistent for all the 18 realizations. However, using the proposed SK thresholding technique the consistency of SK along all the realizations is clearly observed.

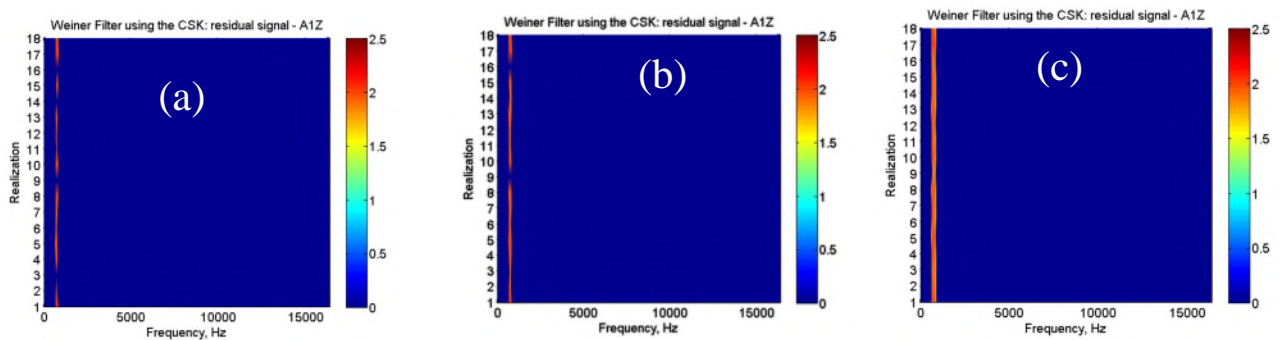


Figure 3: Optimal Wiener Filter obtained using SK thresholding for different values of the consistency parameter by using the proposed thresholding technique (a) $p = 77.77\%$ ($SK_{Th} = 3.7$) (b) $p = 88\%$ ($SK_{Th} = 3.6$) and (c) $p = 100\%$ ($SK_{Th} = 3.5$).

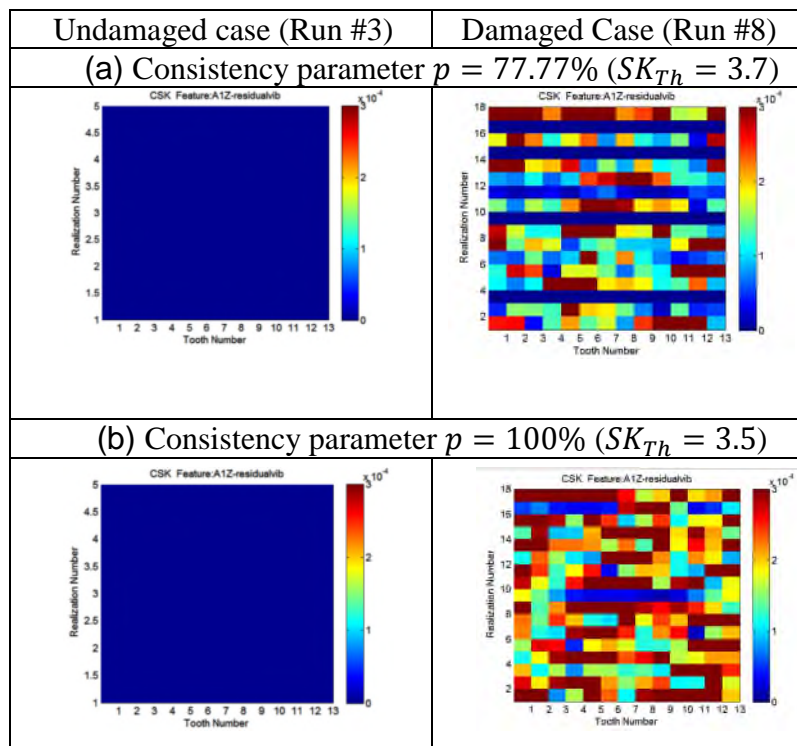


Figure 4: Diagnostic feature of mean squared envelope for each tooth for undamaged (left) and damaged (right) case using CSK technique for consistency levels.

Due to the presence of the inconsistent frequency bands false alarms are expected during the decision making procedure using the statistical thresholding. In the following section the decision making results for the diagnosis decision making are presented.

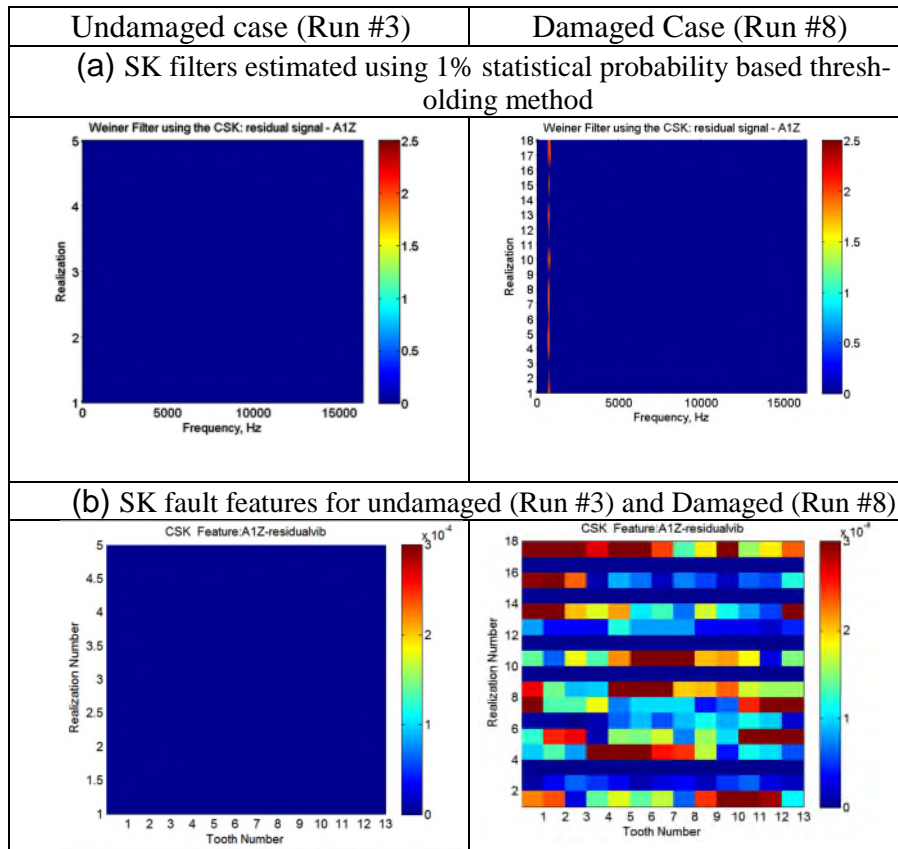


Figure 5: (a) SK filters estimated using 1% statistical probability based thresholding method and (b) Diagnostic feature of mean squared envelope for each tooth for undamaged (left) and damaged (right) case using CSK technique.

3.1.3 Diagnosis decision making

The implemented decision making method is the supervised classification method based on the modified non-parametric kNN approach. The implemented method consists of the following preliminary steps:(1) Data Clusterization - training, and (2) Calculation of the novelty scores – testing. For training purposes, the data were prepared by extracting the features from the undamaged case. This is followed by establishment of the training clusters using the k-means method, and calculation of the averaged distances to k nearest neighbours (the averaged kNN distance) for each sample in each cluster of the training data. Decision-making procedure is based on the comparison of novelty scores with a detection threshold. The test data sample is believed to be the single anomaly when all novelty scores exceed the distance threshold, otherwise it is believed that no anomaly detected. The proposed anomaly detection approach is able to perform decision making independently for each tooth, as the diagnostic features are extracted for each tooth as well. The SK features corresponding to Run #2 and Run #3 (undamaged data) are chosen for training purpose. The decision making results corresponding to two SK thresholding techniques are presented in the figure below. The train-

ing data is classified into 6 numbers of clusters and a k-Nearest Neighbour (kNN) value of 7 is chosen for this study.

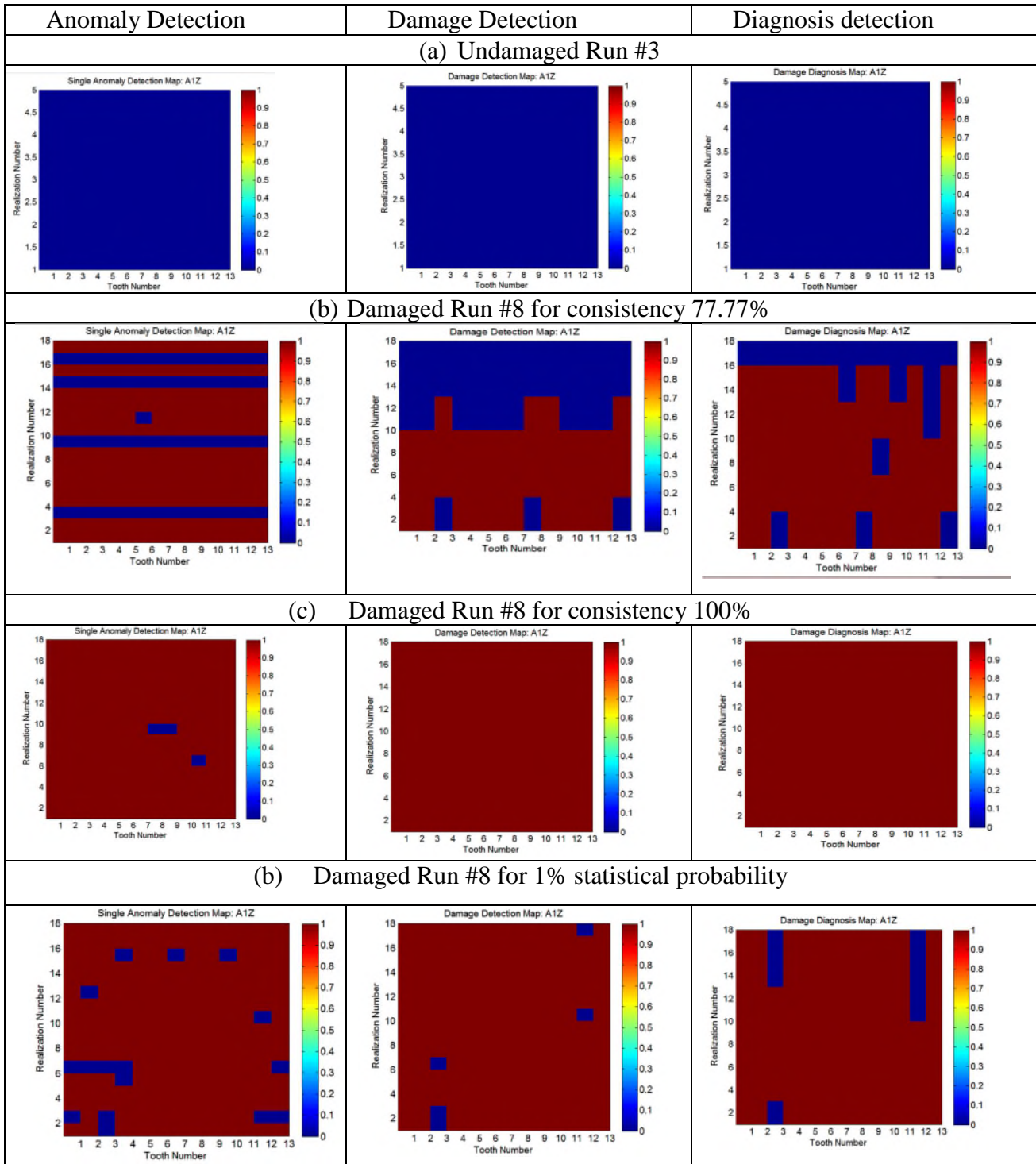


Figure 6: CSK based Diagnosis decision making and the estimated probability of correct diagnosis is (b) For $p=77.77\%$ is 83%, (c) For $p=100\%$ is 100% and (d) For 1% statistical threshold the probability of correct diagnosis is 93%.

In the anomaly detection stage of the undamaged case as shown in Fig.7(a) no false alarms were observed; these false alarms if present are eliminated in the damage detection and damage diagnosis

stages. As shown in Figure 6 for the anomaly detection stage non-anomalous detections were observed. By grouping these detections and by applying weighted majority rule as explained in [6] the damage detection matrix is realized. The grouping procedure is repeated again on the damage detection matrix to obtain the final damage diagnosis matrix which is used for diagnosis decision making. For 1% statistical SK thresholding technique, applied for damaged data the diagnosis decision making results are presented in Figure 6. For 1% SK threshold the probability of correct diagnosis is 93%. For 77.77% consistency level the SK has shown 83.33% probability of correct diagnosis. However, using the proposed technique for CSK fault features, the probability of correct diagnosis is estimated as 100% as shown in Figure 6.

4. Conclusions

The proposed SK thresholding technique is based on maximization of the SK estimate for estimating the optimal Weiner filter. In this paper two SK thresholding techniques are compared based on the diagnosis performance using a three stage decision making technique. The Statistical SK thresholding technique available in literature is based on the probability distribution of the SK estimate. The probability based SK thresholding technique does not ensure consistence of the SK frequency bands. For 1% probability CSK threshold the probability of correct diagnosis is 93% whereas using the proposed CSK thresholding technique the probability of correct diagnosis is 100%. For 100% consistency level using the probability of correct diagnosis is 100%. High level of consistency is desired for SK filtering procedure. The proposed technique ensures that the SK filter estimated is consistent along all the SK realizations. Due to the presence of the inconsistent frequency bands false alarms are expected during the decision making procedure using the statistical thresholding. Also it is observed that for the experimental data estimating the coefficient of threshold $u_{1-\alpha}$ for statistical SK threshold estimation unstable when the signal filtered has low kurtosis, which is often the case for pitting fault tooth damage.

REFERENCES

1. Antoni, J. and Randall, R.B. The spectral kurtosis: application to the vibratory surveillance and diagnostics of rotating machines, *Mechanical Systems and Signal Processing*, **20** (2), 308 – 331, (2006).
2. Antoni, J. The spectral kurtosis: a useful tool for characterising non-stationary signals, *Mechanical Systems and Signal Processing*, **20** (2), 282 – 307, (2006).
3. Valeriu, D. V., Pierre, G. and Christine, S. Spectral Kurtosis: from definition to application, *6th IEEE international workshop on nonlinear signal and image processing (NSIP)*, Grado-Italy, (2003).
4. Yanxue, W. and Ming, L. Identification of multiple transient faults based on the adaptive spectral kurtosis method, *Journal of sound and Vibration*, **331** (2), 470-486, (2012).
5. Combet, F., and Gelman, L., An automated methodology for performing time Synchronous averaging of a gearbox signal without speed sensor, *Mechanical Systems and Signal Processing*, **21**(6), 2590-2606, (2007).
6. Gelman, L., Murray, B., Patel T. H., and Thomson, A. Novel decision making technique for damage diagnosis, *Insight*, **55**(8), 428-432, (2013).

Novel gear diagnosis technique based on spectral kurtosis

Chandra, Harish

2016-07-31

Harish Chandra and Len Gelman. Novel gear diagnosis technique based on spectral kurtosis. 23rd International Congress on Sound and Vibration: From Ancient to Modern Acoustics, (ICSV 2016) 10-14 July 2016, Athens, Greece.

http://www.iiav.org/archives_icsv_last/2016_icsv23/content/papers/papers/full_paper_901_20160603143511560.pdf

Downloaded from CERES Research Repository, Cranfield University